

Analysis of trophic networks: an optimisation approach

Jean-Guy Caputo^{*1}, Valerie Girardin^{†2}, Arnaud Knippel^{‡1}, Hieu Nguyen^{§1}, Nathalie Niquil,^{¶3} and Quentin Noguès,^{||3}

¹Laboratoire de Mathématiques, INSA de Rouen Normandie, 76801 Saint-Etienne du Rouvray, France.

²UNICAEN, CNRS, Laboratoire de Mathématiques Nicolas Oresme, 14000 Caen, France

³UNICAEN, Laboratoire Biologie des ORganismes et Ecosystèmes Aquatiques, FRE 2030 BOREA (MNHN, UPMC, UCBN, CNRS, IRD-207) CS 14032, 14000 Caen, France

October 26, 2021

Abstract

We introduce a methodology to study the possible matter flows of an ecosystem defined by observational biomass data and realistic biological constraints. The flows belong to a polyhedron in a multi dimensional space making statistical exploration difficult in practice; instead, we propose to solve a convex optimization problem. Five criteria corresponding to ecological network indices have been selected to be used as convex goal functions. Numerical results show that the method is fast and can be used for large systems. Minimum flow solutions are analyzed using flow decomposition in paths and circuits. Their consistency is also tested by introducing a system of differential equations for the biomasses and examining the stability of the biomass fixed point. The method is illustrated and explained throughout the text on an ecosystem toy model. It is also applied to realistic food models.

keywords : Convex optimization Ecosystem Trophic network
AMS classification: 92C42, 49N30

*caputo@insa-rouen.fr

†valerie.girardin@unicaen.fr

‡arnaud.knippel@insa-rouen.fr

§mingxiao13492@gmail.com

¶nathalie.niquil@unicaen.fr

||quentin.nogues@unicaen.fr

Acknowledgements This work is part of the ECUME project, co-financed by the European Union with the European regional development fund (ERDF) and by the Normandie Regional Council.

1 Introduction

Functional ecology is based on seminal works from the XXth century centered on the object ecosystem. From the first definition of an ecosystem by [40] to the construction of its main concepts by [26], [34] or [28], among others, ecosystems have been described as entities gathering living organisms and their habitat, and described as dynamic entities, based on exchanges of organic matter. From those works were derived a system analysis of these exchanges based on emergent properties; see [35], [36], [41], [12].

The description of ecosystems is often based on networks of interactions, of different types. For terrestrial ecosystems, recent developments concern different types of interactions, sometimes gathered into a common model called multiplex [10]. In marine ecology, the most studied interactions are trophic, i.e. the interactions between predators and preys; they form a network called a *food web*. Food webs in marine ecosystem are highly complex, compared to the terrestrial ones [1] and have been described by numerous models. These models have been widely used to describe the impact of human activities on marine ecosystems [19]. They are also important tools for the sustainable management of marine and coastal environments [24].

The trophic modeling of food webs has been mainly based on weighted networks; see for example the Ecopath-Ecosim-Ecospace models [6]. There, each link corresponds to a transfer of organic matter between two trophic compartments, collecting individuals of similar feeding behaviors and metabolisms, and with the same predators. Some fluxes can be estimated using laboratory experiments that are often associated to field studies, however many of them remain unknown. To take into account these unknown flux values within food webs, a class of models was developed called Linear Inverse Modeling (LIM) [32]. LIM assumes a steady state for the biomass of all compartments – a mass balanced system. This yields a set of linear equations (equalities) describing the steady state or mass balance. Then, constraints are added from field measurements of mass transfers like local estimations of primary production, respiration or diet contents. Additional constraints come from experiments or the study of other ecosystems. All these constraints constitute a set of linear equalities and inequalities defining a bounded multidimensional polyhedron, called a polytope, within which lie all realistic solutions to the problem. Such solutions are termed flows in graph theory.

In the literature on ecosystems, the polytope is explored using a random walk method, called Monte Carlo Markov Chain – see [21],[22], [44] and [45] – or Monte Carlo Linear Inverse Modeling (MC-LIM) – see [21] and [44]. Linear

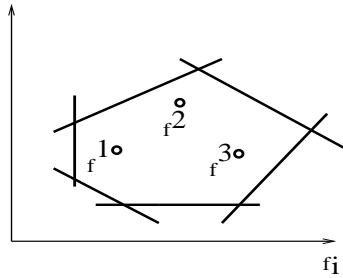


Figure 1: Schematic drawing of the polytope with the optima for different goal functions.

Inverse Monte Carlo Markov Chain (LIM-MCMC) models are mass balanced. This stochastic approach is an indirect way to consider the variability of the living; see [32] [45]. As such, they provide a wide range of possible results, and not a single value like other approaches. However, for large systems, this exploration of the polytope can be very long, with a very large number of simulation runs.

Gathering indices from various domains, from information theory to input-output analysis in econometry, several Ecological Network Analysis indices have been introduced for describing the organization of the flows and the functioning of the ecosystem [25], or as criteria of ecosystem maturity [42]; One such simple index is the sum of the flow components squared [46]; see [18], [22], [38], and [43] for many others. These indices assume that the flows are given, but LIM results can be used to compute approximated values.

In this article, we propose to use these indices as goal functions and combine them with the constraints to set up an optimization problem. This procedure has a low computing time compared to the LIM MC-MC method and directly yields a unique flow solution within the polytope, if the goal function is convex. Note that [38] combined the LIM-MCMC exploration of the polytope to comparison of different indices to select a unique flow vector.

Fig. 1 presents a schematic picture of the polytope in flow space f together with three minima corresponding to three convex goal functions. To compare the optima obtained through optimization of goal functions, say f^1 , f^2 and f^3 , a first step is to examine the main flows from an ecological point of view and see if they appear reasonable. In a more quantitative approach, one can decompose these flows into paths and circuits and again check these using ecology know-how. We also suggest, using simple rules, to introduce a dynamical system satisfied by the biomasses and whose coefficients depend on the flow solution f^1 , f^2 or f^3 . This dynamical system has a fixed point – the given biomasses, whose stability can be determined. If the fixed point is stable, then the model

is consistent, say for example f^2 in Fig. 1. Then the optimum f^2 yields an acceptable solution to describe the ecosystem.

Using a six species toy model inspired by a realistic ecosystem, we proceed to illustrate this methodology. We do not pretend that the model is realistic but we focus on the analysis and present it in as much detail as possible. This detailed presentation is easy to follow on the six species system and naturally extends to an ecosystem of any size. We write explicitly the constraints defining the polytope in Section 2. In Section 3, we discuss flow decomposition into paths and circuits, a general result from the theory of polyhedra. The full optimization problem is presented in Section 4. First we present the five convex goal functions, three of which are independent of the constraints and two depend on the constraints. The results of the optimization problem are analyzed using the flow decomposition of Section 3. From these flow solutions, we write the formal dynamical system for the biomasses and examine the stability of the fixed point in Section 5. We show that the fixed point is always marginally stable, in the absence of detritus, in Section 6. We show that the detritus controls the stability and give a sufficient condition for the fixed point to be stable. Conclusions and application to real data are presented in Section 7.

2 The model and notation

A realistic model of a marine ecosystem with nineteen species was introduced and analyzed by the authors in [33]. To focus on the method of analysis, we simplified this model and reduced it to an ecosystem of six species. This methodology can be extended to ecosystems of arbitrary size; in Section 6, we give some results for the realistic ecosystem studied in [33].

The graph of this simplified 6-species ecosystem is presented in Fig. 2. The ordered types of living organisms with biomasses – circles in Fig. 2 – are:

Phytoplankton \equiv PHY1, Zooplankton \equiv ZOO3, Bivalve \equiv BIV4,
 Fish benthic feeders \equiv FBF5, Bacteria \equiv BAC6.

The other vertices – rectangular boxes in Fig. 2 – are:

Detritus \equiv DET2, Photosynthesis of phytoplankton \equiv FIX7,
 Respiration \equiv RES9, Fishing, Trawl, Dredge,... \equiv LOS10,
 Import to system (ability of a species to move geographically
 in order to feed) \equiv IMP8.

The arrows between the compartments (edges between vertices) represent matter flows that are inferred by ecologists. Following graph theory, terminology such oriented edges will be denoted arcs.

We denote by S the set of all vertices including the detritus DET2,

$$S = \{PHY1, DET2, ZOO3, BIV4, FBF5, BAC6\},$$

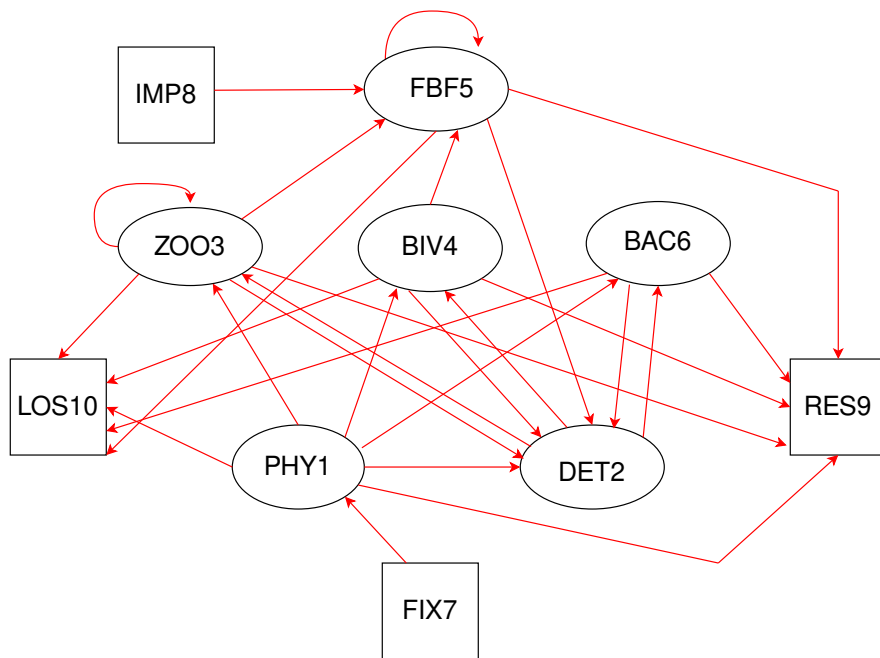


Figure 2: The 6-species model ecosystem described in Section 2.

with $S' = S - \{DET\}$ the set of all species vertices, and E the set of all arcs – denoted by ij when going from vertice i to vertice j .

The central mathematical object of this article is the flow.

Definition 2.1 *Let the successors and predecessors of a vertice i be $N^+(i) = \{\text{vertices } j, ij \in E\}$ and $N^-(i) = \{\text{vertices } j, ji \in E\}$.*

A flow is a vector, of dimension the number of arcs with non negative components, satisfying Kirchoff law on all vertices of S ,

$$\sum_{j \in N^+(i)} f_{i,j} - \sum_{j \in N^-(i)} f_{j,i} = 0, \quad i \in S, \quad (1)$$

In many situations, all biomasses B_i of the species i can be measured with accuracy. On the other hand, the flow components $f_{i,j}$ are much more difficult to evaluate. Therefore, we will adopt here the standard viewpoint that the biomasses are given and the flows between nodes are unknown.

2.1 Biological constraints

The flow components $f_{i,j}$ between the compartments satisfy biological constraints. For example, a fish cannot eat more than a certain percentage of its biomass. When defining the constraints, we gather all available information, if possible from studies of the local ecosystem, if not, from ecosystems similar to ours. In absence of information, the constraints are derived from experiments or from empirical equations.

Definition 2.2 *For all species $i \in S$, the production P_i is*

$$P_i = \sum_{j \in S'} f_{j,i} - f_{i,\text{res}} - f_{i,\text{det}},$$

where $f_{i,\text{res}}$ is the respiration flow and $f_{i,\text{det}}$ is the excretion flow – assuming it goes to the detritus.

Among non species compartments (vertices), the detritus plays a singular role as the only one for which flows go in and out of. It is then natural to assume for it a Kirchoff law where in-going equal out-going flows. For the species vertices in S' , the following constraints are imposed by biological observations through nonnegative coefficients c . These coefficients come from field measurements of mass transfers like local estimations of primary production, respiration or diet contents. They can also be estimated from experiments or the study of other ecosystems.

Positivity of the flow components $f_{i,j} \geq 0$, for all $ij \in E$.

Kirchoff law at the vertices Equations (1) express the conservation of mass at each species vertex.

Primary production constraint The production P_1 of the entry in the ecosystem Phy1 is bounded,

$$c_{\text{pro}}^- \leq P_1 \leq c_{\text{pro}}^+.$$

This constraint comes from a local study estimating the carbon incorporated, with enrichments in ^{13}C a stable isotope of carbon, compared with studies based on an estimation of the activity of photosystems using pulse amplitude modulation [30].

Respiratory constraints The respiration flow $f_{i,\text{res}}$ of each species i is bounded,

$$c_{\text{res},i}^- \sum_{j \in N^-(i)} f_{j,i} \leq f_{i,\text{res}} \leq c_{\text{res},i}^+ \sum_{j \in N^-(i)} f_{j,i}, \quad \text{for all } i \in S'.$$

Excretion constraints The excretion of all species i but the phytoplankton is bounded,

$$c_{\text{det},i}^- \sum_{j \in N^-(i)} f_{j,i} \leq f_{i,\text{det}} \leq c_{\text{det},i}^+ \sum_{j \in N^-(i)} f_{j,i}, \quad \text{for all } i \in S', i \neq \text{PHY1}.$$

The phytoplankton excretion is bounded too,

$$c_{\text{det,phy}}^- P_{\text{phy}} \leq f_{\text{phy,det}} \leq c_{\text{det,phy}}^+ P_{\text{phy}}.$$

Food conversion efficiencies constraints The production of a species i is constrained by bounds depending on the entering flow of species i

$$c_{\text{eff},i}^- \sum_{j \in N^-(i)} f_{j,i} \leq P_i \leq c_{\text{eff},i}^+ \sum_{j \in N^-(i)} f_{j,i}, \quad \text{for all } i \in S'.$$

Production related to biomass constraints The production of a species i is constrained by bounds depending on its biomass B_i ,

$$c_{\text{bio},i}^- B_i \leq P_i \leq c_{\text{bio},i}^+ B_i, \quad \text{for all } i \in S',$$

Diet constraints The entry flow $f_{j,i}$ for species i is constrained by bounds depending on the sum of the entry flow of this species,

$$c_{\text{diet},i}^- \sum_{j \in N^-(i)} f_{j,i} \leq f_{j,i} \leq c_{\text{diet},i}^+ \sum_{j \in N^-(i)} f_{j,i}, \quad \text{for all } i \in S'.$$

Diet information is derived from stomach content analyses; see e.g. [9].

Different empirical equations are gathered to define relationships between production and biomass or consumption and biomass, or respiration and consumption; see [3], [11]. These equations use the shape of the caudal fin, the individual weight, temperature, growth, etc. The individual mass and total biomass per km² values are estimated from local field studies [8] or field studies from a similar ecosystem if not available; see, e.g., for zooplankton [37].

All above constraints can be summarized in the following set of equations, where f_i is the total flow entering a species i .

$$f_{i,j} \geq 0, \quad ij \in E, \quad (2)$$

$$f_i = \sum_{j \in N^-(i)} f_{j,i}, \quad i \in S, \quad (3)$$

$$\sum_{j \in N^+(i)} f_{i,j} - \sum_{j \in N^-(i)} f_{j,i} = 0, \quad i \in S, \quad (4)$$

$$f_1 - f_{1,\text{res}} - f_{1,\text{det}} - c_{\text{pro}}^+ \leq 0, \quad (5)$$

$$-f_1 + f_{1,\text{res}} + f_{1,\text{det}} + c_{\text{pro}}^- \leq 0, \quad (6)$$

$$-c_{\text{res},i}^+ f_i + f_{i,\text{res}} \leq 0, \quad i \in S', \quad (7)$$

$$c_{\text{res},i}^- f_i - f_{i,\text{res}} \leq 0, \quad i \in S', \quad (8)$$

$$-c_{\text{det},i}^+ f_i + f_{i,\text{det}} \leq 0, \quad i \in S', i \neq \text{PHY1} \quad (9)$$

$$c_{\text{det},i}^- f_i - f_{i,\text{det}} \leq 0, \quad i \in S', i \neq \text{PHY1} \quad (10)$$

$$-c_{\text{det,phy}}^+ P_{\text{phy}} + f_{\text{phy,det}} \leq 0, \quad (11)$$

$$-f_i + f_{i,\text{res}} + f_{i,\text{det}} + c_{\text{eff},i}^- f_i \leq 0, \quad i \in S', \quad (12)$$

$$f_i - f_{i,\text{res}} - f_{i,\text{det}} - c_{\text{bio},i}^+ B_i \leq 0, \quad i \in S', \quad (13)$$

$$-f_i + f_{i,\text{res}} + f_{i,\text{det}} + c_{\text{bio},i}^- B_i \leq 0, \quad i \in S', \quad (14)$$

$$f_{j,i} - c_{\text{diet},i,j}^+ f_j \leq 0, \quad j \in S, i \in S', \quad (15)$$

$$-f_{j,i} + c_{\text{diet},i,j}^- f_j \leq 0, \quad j \in S, i \in S'. \quad (16)$$

For the 6-species ecosystem defined in Fig. 2, these constraints lead to the bounds on the flows shown in Table 1. More precisely, for example, the bounds on $f_{1,2}$ are obtained by minimizing or maximizing $f_{1,2}$ together with the constraints (2) to (16).

3 Flow decomposition

Since the constraints (2) to (16) are all linear, the defined domain is polyhedral. A polyhedron in \mathbb{R}^n is an intersection of a finite number of half-spaces, in other words $P = \{x \in \mathbb{R}^n | Ax \leq b\}$, where A is an $n' \times n$ matrix with $n' > n$ and $b \in \mathbb{R}^{n'}$. A bounded polyhedron is called a polytope.

The decomposition $P = Q + C$ for all polyhedrons P , with Q a polytope and C a cone, is classical; see Nemhauser and Wolsey [31]. Since Q and C are convex

Components	bounds	Components	bounds
$f_{1,2}$	[10.300 ; 51.600]	$f_{3,2}$	[0.000 ; 82.036]
$f_{1,3}$	[0.000 ; 136.181]	$f_{3,3}$	[0.000 ; 16.407]
$f_{1,4}$	[35.818 ; 172.000]	$f_{3,4}$	[0.000 ; 39.002]
$f_{1,6}$	[0.000 ; 96.498]	$f_{3,5}$	[0.000 ; 35.445]
$f_{1,9}$	[5.963 ; 95.828]	$f_{3,9}$	[0.000 ; 49.222]
$f_{1,10}$	[0.000 ; 129.668]	$f_{3,10}$	[0.000 ; 78.113]
$f_{2,3}$	[0.000 ; 27.892]	$f_{4,2}$	[11.722 ; 111.138]
$f_{2,4}$	[9.768 ; 92.615]	$f_{4,5}$	[0.000 ; 35.445]
$f_{2,6}$	[0.000 ; 271.796]	$f_{4,9}$	[18.235 ; 197.447]
		$f_{4,10}$	[0.000 ; 78.260]
Components	bounds	Components	bounds
$f_{5,2}$	[0.638 ; 35.445]	$f_{6,2}$	[0.000 ; 112.581]
$f_{5,5}$	[0.000 ; 6.380]	$f_{6,9}$	[0.000 ; 180.966]
$f_{5,9}$	[3.190 ; 31.901]	$f_{6,10}$	[0.000 ; 192.996]
$f_{5,10}$	[0.000 ; 6.380]	$f_{7,1}$	[119.263 ; 319.428]
		$f_{8,5}$	[0.000 ; 35.445]

Table 1: Bounds on the flow components for the 6-species ecosystem of Fig. 2.

sets, any point in P can be expressed as the sum of a convex combination of the extreme points of Q (the vertices) and a combination of the extreme rays of C with non negative coefficients :

$$x = \sum_{i \in I} \alpha_i q^i + \sum_{j \in J} \beta_j r^j, \quad (17)$$

where I is the index set of the vertices of Q , J the index set of the extreme rays of C and the coefficients α_i satisfy $\sum_{i \in I} \alpha_i = 1$ and α_i, β_j are non negative.

For webs of flows, the vertices of Q are indicator vectors of elementary paths and the extreme rays are – up to a constant coefficient – indicator vectors of elementary circuits of the web (paths that begin and ends at the same vertex). Therefore any numerical solution of such an ecological system can be interpreted in terms of paths and circuits. A linked important notion is the flow value.

Definition 3.1 *For a given path or circuit, the flow value is the smallest flux for all arcs of the path or circuit.*

Usually, the decomposition (17) is not unique. However, the largest flow values of the network will make some paths or circuits necessary in any decomposition, and hence important for interpreting the obtained ecosystem solution. An algorithm to find all necessary paths or circuits is the following:

Repeat

- Find the path or circuit with largest value α ;

- Take out α from the flow components of the arcs of this path or circuit;

until stopping criterion is met.

Such an analysis assumes that the numerical values of the flows are known and satisfy the biological constraints. Unfortunately, such exact numerical values are generally unavailable, and their a priori approximated values do not satisfy the constraints especially the conservation ones. The next section presents an optimization approach addressing this issue. A flow solution is computed from the knowledge of only the biomasses and some approximated values of the flows, or intervals of approximated values. Then, examples of paths and circuits extracted using the above method of flow decomposition are given for the 6-species network.

4 The Optimization problem

4.1 Goal functions

We consider five goal functions, the most classical least squares, Ecological Network Analysis indices, and functions adapted from information theory. All are convex, yielding a unique optimum corresponding to a unique functioning state of the system. An important characteristic is whether the goal function includes information from the constraints or not. This separates the functions in two classes.

In one class, no information is used from the constraints. The first function corresponds to the quadratic energy, the classical least squares method, and the solution will be the minimum of

$$F_1(f) = \sum_{ij \in E} f_{i,j}^2. \quad (18)$$

The second function is minus Shannon entropy from information theory [5], introduced for ecological systems in 1955 in [28],

$$F_2(f) = \sum_{ij \in E} p_{i,j} \ln(p_{i,j}) = \sum_{ij \in E} \frac{f_{i,j}}{f_{..}} \ln \left(\frac{f_{i,j}}{f_{..}} \right), \quad (19)$$

where the sum of all flows is $f_{..} = \sum_{ij \in E} f_{i,j}$, and the proportion of flows from vertex i to vertex j is

$$p_{i,j} = \frac{f_{i,j}}{f_{..}}. \quad (20)$$

Classically, entropy is a concave function and is to be maximized. Here, for practical purposes, we only deal with convex goal functions and therefore changed the sign. With this sign, F_2 is convex – see Appendix 2.

Finally, the third function is minus the system redundancy (overhead) introduced in [42] as

$$F_3(f) = \sum_{ij \in E} p_{i,j} \ln \left(\frac{p_{i,j} p_{i,j}}{p_{i.} p_{.j}} \right) = \sum_{ij \in E} \frac{f_{i,j}}{f_{..}} \ln \left(\frac{f_{i,j}^2}{f_{i.} f_{.j}} \right), \quad (21)$$

where the marginal proportions are

$$p_{i.} = \sum_{j \in S: ij \in E} p_{i,j} \quad \text{and} \quad p_{.j} = \sum_{i \in S: ij \in E} p_{i,j};$$

note that the sum is on all i or j such that ij is an arc of E . As for the entropy, with this choice of sign, F_3 is convex – see Appendix 2.

In information theory terms, $-F_2$ is the Shannon entropy of the system and $-F_3$ is a symmetrized conditional entropy; see [5] and also [43] for details on such entropic indexes. Note that, although it is a well-known Ecological Network Analysis index, we do not consider the ascendancy of [15] because it is neither convex nor concave – see Appendix 2.

In the other class, the goal functions incorporate information from the constraints. The most classical quantity in this aim in information theory is the Kullback-Leibler divergence introduced in [23], that measures a "distance" between two distributions,

$$F_4(f) = K(f|f^*) = \sum_{ij \in E} p_{i,j} \ln \left(\frac{p_{i,j}}{p_{ij}^*} \right), \quad (22)$$

where the proportions are given in (20). The divergence is not a mathematical distance because it is not symmetric in p and p^* . Still, it is nonnegative and null only if $p = p^*$, and minimizing K determines the projection in terms of divergence of the reference f^* (or p^*) on the set of solutions f to the constraints; see [5] and [7]. A natural way, that makes sense in ecology, to include the information from the constraints is to set all f_{ij}^* as the middle of the constraint intervals $[f_{ij}^{\min}, f_{ij}^{\max}]$. Note that F_2 is the Kullback-Leibler divergence where f^* is the uniform distribution on the flows. This uniform distribution is usually not a flow; this confirms the importance of using graph theory to describe such systems.

Finally, a simple generalization of the quadratic function F_1 is

$$F_5(f) = \sum_{ij \in E} (f_{i,j} - f_{i,j}^*)^2. \quad (23)$$

4.2 The full optimization problem

Combining the biological constraints (2) to (16) with the goal functions (18) to (23) yields the well posed convex optimization problem in a positive polytope

of \mathbb{R}^n ,

$$\begin{aligned} \min_f F, \\ \text{with constraints (2) – (16),} \end{aligned} \tag{24}$$

where F can be any one of the five goal functions given in (18) to (23).

A well suited method to solve (24) is the Sequential Quadratic Programming (SQP) which uses an Augmented Lagrangian Solver; see [2] contained in the R library Nloptim [4]. We used the R software infrastructure for the optimization. The algorithm is presented in Appendix 1.

The flows corresponding to the optimum for the five different goal functions and the 6-species ecosystem are presented in Table 2. Using the flow decomposition estimation introduced in the previous section, we computed the main paths and the circuits for each flow solution. These are shown respectively in black and green in Fig. 3.

For instance for the graph minimizing F_1 , the main paths/circuits are:

$$\begin{aligned} \text{FIX7} &\xrightarrow{33} \text{PHY1} \xrightarrow{33} \text{LOS10}, \\ \text{FIX7} &\xrightarrow{29} \text{PHY1} \xrightarrow{29} \text{BIV4} \xrightarrow{29} \text{RES9}, \\ \text{BIV4} &\xrightarrow{17} \text{DET2} \xrightarrow{17} \text{BIV4}. \end{aligned} \tag{25}$$

Fig. 3 shows the graph with the largest obtained flows. The flows obtained for F_4 and F_5 appear as the most expected results as the largest flow components are located at the low trophic levels, corresponding to the classical pyramidal view of energy flows proposed by [26] and [17].

Note that the common path (25) appears for the five optimization functions, showing the well-known importance of phytoplankton in coastal ecosystems. This path is the main input of energy in the system. Pathways with largest flows also display the role of the bivalves in the system: they are important consumers of phytoplankton and producers of detritus. Their role as recyclers shows in solutions for all goal functions. In such ecosystems, bivalves are not the only recyclers, bacteria also recycle through the bacterial loop. This shows in solutions yielded by F_4 and F_5 . One odd path is the importation path to fish FBF in the solution of F_2 ; its importance displays a state of the food web where the connection to other systems is crucial for the high trophic level FBF compartment. This solution corresponds to an extreme case, where the system is unable to sustain the FBF compartment and thus relies more on importation.

Component	Solution 1	Solution 2	Solution 3	Solution 4	Solution 5
$f_{1,2}$	10.300	10.300	10.940	15.924	39.948
$f_{1,3}$	25.469	45.800	41.130	44.577	51.098
$f_{1,4}$	38.784	36.175	35.818	55.847	83.598
$f_{1,6}$	5.272	13.237	14.186	25.257	27.971
$f_{1,9}$	5.963	7.907	16.766	18.026	29.146
$f_{1,10}$	33.472	7.787	12.040	21.268	9.331
$f_{2,3}$	4.499	7.722	6.576	6.515	10.465
$f_{2,4}$	17.814	23.020	22.668	26.501	52.497
$f_{2,6}$	12.302	50.156	33.101	70.547	140.374
$f_{3,2}$	5.993	12.382	9.910	19.171	30.782
$f_{3,3}$	0.000	1.658	1.847	2.614	0.000
$f_{3,4}$	8.525	6.577	6.638	8.270	15.900
$f_{3,5}$	3.244	11.057	9.144	5.068	5.322
$f_{3,9}$	8.990	15.208	14.866	7.682	6.156
$f_{3,10}$	3.213	8.297	7.147	10.899	3.402
$f_{4,2}$	16.542	18.746	18.165	27.340	58.398
$f_{4,5}$	4.508	11.591	10.462	6.327	10.692
$f_{4,9}$	29.045	27.294	27.421	41.977	74.061
$f_{4,10}$	15.028	8.212	9.075	14.973	8.845
$f_{5,2}$	0.901	21.596	10.197	12.091	22.394
$f_{5,5}$	1.232	3.834	3.513	2.278	6.380
$f_{5,9}$	5.681	24.845	16.380	8.072	16.014
$f_{5,10}$	1.201	2.545	2.866	1.741	0.000
$f_{6,2}$	0.878	17.874	13.131	29.036	51.814
$f_{6,9}$	8.384	22.759	20.390	32.476	55.258
$f_{6,10}$	8.384	22.759	13.766	34.310	61.273
$f_{7,1}$	119.263	121.207	130.883	180.919	241.095
$f_{8,5}$	0.031	26.411	9.838	10.508	22.394

Table 2: Flow solutions for the 6-species system, obtained for the goal functions F_1 to F_5 .

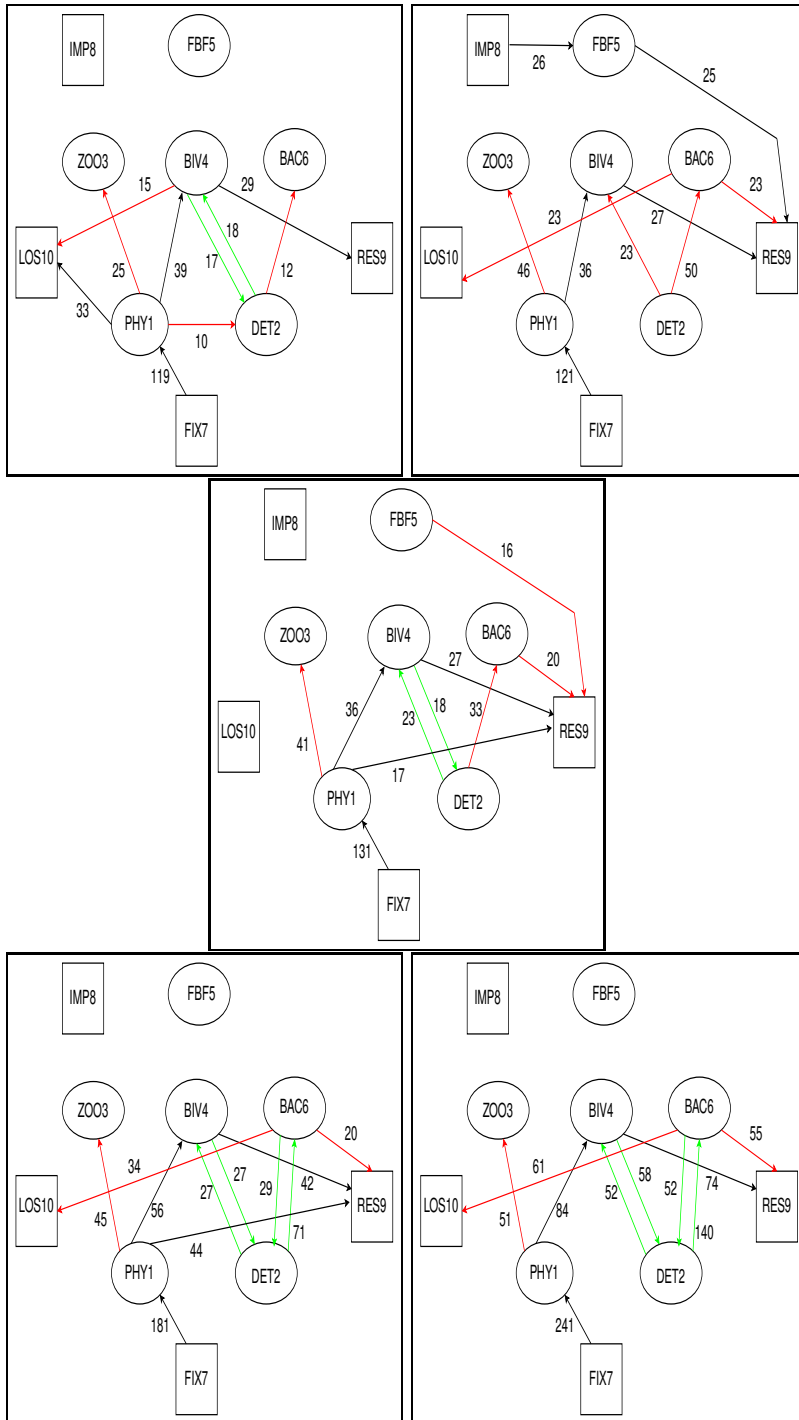


Figure 3: The largest flows for the 6-species system and the goal functions: **top** F_1 (left) and F_2 (right), **middle** F_3 , **bottom** F_4 (left) and F_5 (right). Red lines are paths and green lines are circuits. 14

5 Consistency of the solution: stability of the ecosystem

Solving the optimization problem (24) for each goal function F_i yields a series of flows f between the species (including detritus) vertices. From these flows, using a set of biological rules to be given below, we obtain a formal dynamical system where the variables are the biomasses B_i . This system involves coupling coefficients α that will differ for the different goal functions.

All these systems have, by construction, the same fixed point corresponding to the given biomasses. Then, by examining the eigenvalue with maximal real part of the Jacobians of these different dynamical systems at the fixed point, we can evaluate the structural stability of the ecosystem for this set of biomasses.

5.1 The dynamical system

Each flow solution f of the optimization problem (24) can be used to derive a system of differential equations satisfied by the biomasses. The following rules will be used to derive these systems of differential equations.

If living organisms of species i eat organisms of (either living or detritus) species j , the flow $f_{i,j}$ is given by a law of mass action or Lotka-Volterra coupling – see [29],

$$f_{i,j} = \alpha_{i,j} B_i B_j. \quad (26)$$

Other flows are assumed to be proportional to the biomass of the start vertex, with a coefficient of proportionality depending also on the finish vertex,

$$f_{i,j} = \alpha_{i,j} B_i. \quad (27)$$

Thus, the dynamics of the system is given by the flow $f = (f_{i,j})$, that is to say by $\alpha = (\alpha_{i,j})$.

For the 6-species ecosystem of Fig. 2, the formal rules (26) and (27) lead to the system of differential equations

$$\dot{B}_1 = f_{7,1} - f_{1,9} - f_{1,2} - f_{1,4} - f_{1,3} - f_{1,6} - f_{1,10}, \quad (28)$$

$$\dot{B}_2 = f_{1,2} + f_{6,2} + f_{3,2} + f_{4,2} + f_{5,2} - f_{2,4} - f_{2,3} - f_{2,6}, \quad (29)$$

$$\dot{B}_3 = f_{2,3} + f_{1,3} - f_{3,9} - f_{3,2} - f_{3,5} - f_{3,4} - f_{3,10}, \quad (30)$$

$$\dot{B}_4 = f_{2,4} + f_{1,4} + f_{3,4} - f_{4,9} - f_{4,2} - f_{4,5} - f_{4,10}, \quad (31)$$

$$\dot{B}_5 = f_{8,5} + f_{3,5} + f_{4,5} - f_{5,9} - f_{5,2} - f_{5,10}, \quad (32)$$

$$\dot{B}_6 = f_{2,6} + f_{1,6} - f_{6,9} - f_{6,2} - f_{6,10}. \quad (33)$$

By construction, the fixed point of the dynamical system is obtained at the

Cost function	F_1	F_2	F_3	F_4	F_5
$\max(\mathcal{R}\epsilon(\lambda))$	0.093	0.021	0.104	0.149	-0.193

Table 3: Maximum values of the real parts of the eigenvalues of the Jacobian associated to the five goal functions for the 6-species ecosystem.

known biomasses of the 6-species ecosystem,

$$B_1^0 = 3.24, B_2^0 = 19, B_3^0 = 1.72, B_4^0 = 19.5, B_5^0 = 3.19, B_6^0 = 0.75. \quad (34)$$

At the equilibrium point $\dot{B}_i = 0$ for all i , and we get, using (28)-(33),

$$\begin{aligned} \alpha_{7,1}B_1 - \alpha_{1,9}B_1 - \alpha_{1,2}B_1 - \alpha_{1,4}B_1B_4 - \alpha_{1,3}B_1B_3 - \alpha_{1,6}B_1B_6 - \alpha_{1,10}B_1 &= 0, \\ \alpha_{1,2}B_1 + \\ \alpha_{6,2}B_6 + \alpha_{3,2}B_3 + \alpha_{4,2}B_4 + \alpha_{5,2}B_5 - \alpha_{2,4}B_2B_4 - \alpha_{2,3}B_2B_3 - \alpha_{2,6}B_2B_6 &= 0, \\ \alpha_{2,3}B_2B_3 + \\ \alpha_{1,3}B_1B_3 - \alpha_{3,9}B_3 - \alpha_{3,2}B_3 - \alpha_{3,5}B_3B_5 - \alpha_{3,4}B_3B_4 - \alpha_{3,10}B_3 &= 0, \\ \alpha_{2,4}B_2B_4 + \\ \alpha_{1,4}B_1B_4 + \alpha_{3,4}B_3B_4 - \alpha_{4,9}B_4 - \alpha_{4,2}B_4 - \alpha_{4,5}B_4B_5 - \alpha_{4,10}B_4 &= 0, \\ \alpha_{8,5}B_5 + \alpha_{3,5}B_3B_5 + \alpha_{4,5}B_4B_5 - \alpha_{5,9}B_5 - \alpha_{5,2}B_5 - \alpha_{5,10}B_5 &= 0, \\ \alpha_{2,6}B_2B_6 + \alpha_{1,6}B_1B_6 - \alpha_{6,9}B_6 - \alpha_{6,2}B_6 - \alpha_{6,10}B_6 &= 0. \end{aligned}$$

5.2 Stability of the fixed point

A standard way to compute the stability of the fixed point is to evaluate the eigenvalues of the Jacobian matrix of the system. If the real part of one or more eigenvalues is positive, then the fixed point is unstable.

For the 6-species system, the Jacobian is

$$J = \begin{array}{cccccc} & & & & & (35) \\ \left[\begin{array}{cccccc} 0 & 0 & -\alpha_{1,3}B_1 & -\alpha_{1,4}B_1 & 0 & -\alpha_{1,6}B_1 \\ \alpha_{1,2} & -\alpha_{2,4}B_4 - \alpha_{2,3}B_3 - \alpha_{2,6}B_6 & \alpha_{3,2} - \alpha_{2,3}B_2 & \alpha_{4,2} - \alpha_{2,4}B_2 & \alpha_{5,2} & \alpha_{6,2} - \alpha_{2,6}B_2 \\ \alpha_{1,3}B_3 & \alpha_{2,3}B_3 & 0 & -\alpha_{3,4}B_3 & -\alpha_{3,5}B_3 & 0 \\ \alpha_{1,4}B_4 & \alpha_{2,4}B_4 & \alpha_{3,4}B_4 & 0 & -\alpha_{4,5}B_4 & 0 \\ 0 & 0 & \alpha_{3,5}B_5 & \alpha_{4,5}B_5 & 0 & 0 \\ \alpha_{1,6}B_6 & \alpha_{2,6}B_6 & 0 & 0 & 0 & 0 \end{array} \right] \end{array}$$

Using the optimal solutions obtained in Table 2 for the different goal functions, the biomass values (34), and rules (26) and (27), we can compute the maximal real part of the eigenvalues of J , shown in Table 3.

Table 3 shows that only F_5 yields a stable biomass fixed point. Further, Fig. 4 shows the spectra in the complex plane of the Jacobians for the five goal

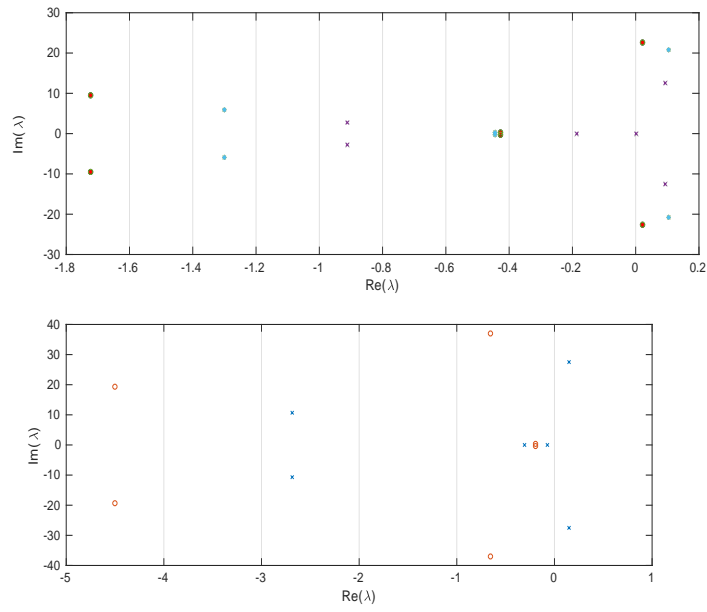


Figure 4: The spectra in the complex plane of the Jacobians for the goal functions: **top** F_1 (black \times), F_2 (red o), F_3 (blue *); **bottom** F_4 (black \times), F_5 (red o).

functions. Again, the systems are unstable for F_1 to F_4 . For all four cases, the eigenvalues with maximum real part are close and have a large imaginary part indicating strong oscillations. These goal functions give rise to similar dynamical behaviors. On the contrary, F_5 gives rise to a weakly stable fixed point with no oscillations. There are then at least two main regions in the parameter space, giving different behaviors.

6 Ecosystem dynamics with or without detritus

From line 2 of the Jacobian J in (35), we see that the detritus acts in a different way than the regular species. To understand this effect, we will detail the equations governing the dynamical systems with and without detritus.

6.1 Lotka-Volterra models for the ecosystem without and with detritus

First, we assume that the detritus species is absent so that we have a pure Lotka-Volterra coupling, of which the theory is well established. Since the considered ecosystem involve no coupling $B_i - B_i$, a Lyapunov function can be found to show that the equilibrium point is (globally) stable. We will follow [27], see also [14].

Consider the Lotka-Volterra model for n species without detritus

$$\frac{dB_i}{dt} = B_i \left(\beta_i + \sum_{j=1}^n \alpha_{ji} B_j \right), \quad i = 1, \dots, n,$$

where $\alpha_{ij} = -\alpha_{ji}$ for all i, j for the couplings (26) and $\beta_i = \sum_j \alpha_{ji}$ for the couplings (27).

The nontrivial equilibrium $(\tilde{B}_1, \dots, \tilde{B}_n)$ is the solution of the system

$$\beta_i + \sum_{j=1}^n \alpha_{ji} B_j = 0, \quad i = 1, \dots, n.$$

This equilibrium is feasible, that is $\tilde{B}_i > 0$, for all i . Moreover, A is a skew-symmetric matrix so that $A + A^T = 0$, where A^T denotes the transpose of A . These two conditions induce that the Lotka-Volterra model is globally stable, see [27].

Thus, the detritus is what will determine the stability. Its in and out flows depend on the goal function.

Let us now consider the system with detritus. The Lotka-Volterra model

with n species including detritus is

$$\begin{aligned}\frac{dB_i}{dt} &= B_i \left(\beta_i + \sum_{j=1}^n \alpha_{ji} B_j \right), \quad i \neq 2, \\ \frac{dB_2}{dt} &= \sum_{i=1, i \neq 2}^n B_i (\alpha_{i2} - \alpha_{2i} B_2),\end{aligned}$$

where B_2 is the biomass of the detritus, $\alpha_{ij} = -\alpha_{ji}$ for all $i, j \neq 2$, $\alpha_{i2} \geq 0$ and $\alpha_{2i} \geq 0$ for all $i \neq 2$.

The Jacobian matrix of this system is

$$J = J^0 + R, \quad (36)$$

where $J_{ij}^0 = \alpha_{ji} B_i$ for all i, j , $R_{2i} = \alpha_{i2}$, and $R_{22} = -\sum_i \alpha_{2i} B_i$, and $R_{ij} = 0$ for $i \neq 2$. One can see that

$$J^0 = DA, \quad (37)$$

where D is the diagonal matrix of biomasses, with $d_{jj} = B_j$, and A is a skew-symmetric matrix.

For example, for the six species system, we have

$$J_0 = \begin{bmatrix} 0 & 0 & -\alpha_{1,3}B_1 & -\alpha_{1,4}B_1 & 0 & -\alpha_{1,6}B_1 \\ 0 & 0 & -\alpha_{2,3}B_2 & -\alpha_{2,4}B_2 & 0 & -\alpha_{2,6}B_2 \\ \alpha_{1,3}B_3 & \alpha_{2,3}B_3 & 0 & -\alpha_{3,4}B_3 & -\alpha_{3,5}B_3 & 0 \\ \alpha_{1,4}B_4 & \alpha_{2,4}B_4 & \alpha_{3,4}B_4 & 0 & -\alpha_{4,5}B_4 & 0 \\ 0 & 0 & \alpha_{3,5}B_5 & \alpha_{4,5}B_5 & 0 & 0 \\ \alpha_{1,6}B_6 & \alpha_{2,6}B_6 & 0 & 0 & 0 & 0 \end{bmatrix} = DA,$$

where

$$D = \begin{bmatrix} B_1 & 0 & 0 & 0 & 0 & 0 \\ 0 & B_2 & 0 & 0 & 0 & 0 \\ 0 & 0 & B_3 & 0 & 0 & 0 \\ 0 & 0 & 0 & B_4 & 0 & 0 \\ 0 & 0 & 0 & 0 & B_5 & 0 \\ 0 & 0 & 0 & 0 & 0 & B_6 \end{bmatrix} \quad \text{and} \quad A = \begin{bmatrix} 0 & 0 & -\alpha_{1,3} & -\alpha_{1,4} & 0 & -\alpha_{1,6} \\ 0 & 0 & -\alpha_{2,3} & -\alpha_{2,4} & 0 & -\alpha_{2,6} \\ \alpha_{1,3} & \alpha_{2,3} & 0 & -\alpha_{3,4} & -\alpha_{3,5} & 0 \\ \alpha_{1,4} & \alpha_{2,4} & \alpha_{3,4} & 0 & -\alpha_{4,5} & 0 \\ 0 & 0 & \alpha_{3,5} & \alpha_{4,5} & 0 & 0 \\ \alpha_{1,6} & \alpha_{2,6} & 0 & 0 & 0 & 0 \end{bmatrix}.$$

Finally, the matrix R is

$$R = \begin{bmatrix} 0 & 0 & 0 & 0 & 0 & 0 \\ \alpha_{12} & -\alpha_{24}B_4 - \alpha_{23}B_3 - \alpha_{26}B_6 & \alpha_{32} & \alpha_{42} & \alpha_{52} & \alpha_{62} \\ 0 & 0 & 0 & 0 & 0 & 0 \\ 0 & 0 & 0 & 0 & 0 & 0 \\ 0 & 0 & 0 & 0 & 0 & 0 \\ 0 & 0 & 0 & 0 & 0 & 0 \end{bmatrix}.$$

6.2 Sufficient condition for stability

Evaluating how the detritus will change the stability of the system is a difficult problem. Nevertheless, perturbation theory can help to understand how eigenvalues of J_0 get displaced to the ones of $J = J_0 + R$ when the norm of R is much smaller than the norm of J_0 , say $\|R\| \ll \|J_0\|$; see [39]. The standard complex inner product on \mathbb{C}^n will be denoted by (\cdot, \cdot) and \bar{z} is the conjugate of z .

Proposition 6.1 *With the notation of the previous section, a sufficient condition for the stability of the system with detritus is*

$$\mathcal{R}e(v^i, Rv^i) \leq 0, \quad i \in S, \quad (38)$$

where the v^i are eigenvectors associated to the eigenvalues λ_0^i of J^0 .

proof We will prove that (38) implies that the real parts of the eigenvalues of J are all negative.

An approximation λ_J^i of an eigenvalue of J is given by

$$\lambda_J^i = \lambda_0^i + \frac{(w^i, Rv^i)}{(w, v^i)}, \quad (39)$$

see [39], where the vector w satisfies

$$J_0^T w = \overline{\lambda_0^i} w. \quad (40)$$

In our special context, the eigenvalues of $J_0 = DA$ are zero or pure imaginary (see Lemma 8.1 in Appendix 3), so that without detritus, the fixed point of the biomasses is marginally stable. The presence of the detritus will shift this stability. Let us prove that $w = D^{-1}v^i$ satisfies (40).

Indeed, since D is invertible, we deduce from $J_0 v^i = DAv^i = \lambda_0^i v^i$ that $Av^i = \lambda_0^i D^{-1}v^i$.

Since $J_0^T = (DA)^T = -AD$, we compute

$$J_0^T w = -ADD^{-1}v^i = -Av^i = -\lambda_0^i D^{-1}v^i = -\lambda_0^i w. \quad (41)$$

Thanks to (37), Lemma 8.1 applies to show that $-\lambda_0^i = \overline{\lambda_0^i}$. Therefore, $J_0^T w = \overline{\lambda_0^i} w$, and $w = D^{-1}v^i$ is an eigenvector of J_0^T , satisfying (40).

Thus, according to (39),

$$\lambda_J^i = \lambda_0^i + \frac{(D^{-1}v^i, Rv^i)}{(D^{-1}v^i, v^i)}.$$

The real parts of λ_0^i are all null, so $\mathcal{R}e(\lambda_J^i) \leq 0$ as soon as

$$\Delta_i \equiv \mathcal{R}e\left(\frac{(D^{-1}v^i, Rv^i)}{(D^{-1}v^i, v^i)}\right) \leq 0.$$

Goal function	F_1	F_2	F_3	F_4	F_5
$\max(\mathcal{Re}(\lambda))$	0.075	0.127	0.242	0.126	0.233

Table 4: Maximum values of the real parts of the eigenvalues of the Jacobian associated to the five goal functions for the 19-species ecosystem.

Since

$$(D^{-1}v^i, v^i) = \sum_{j=1}^n \frac{|v_j^i|^2}{B_j} > 0 \quad \text{for all } i,$$

we only need to consider the sign of the real part of

$$(D^{-1}v^i, Rv^i) = \frac{1}{B_2}(v^i, Rv^i).$$

Then $\Delta_i \leq 0$ if and only if $\mathcal{Re}(v^i, Rv^i) \leq 0$, and (38) is indeed a sufficient condition for the stability of the ecosystem.

7 Discussion and conclusion

Our methodology can easily be applied to general realistic ecosystems with a larger number of species and flow components. To show this, let us present the analysis of the 19-species system defined and studied in [33].

Fig. 5 shows the largest flow components similarly to Fig. 3. As for the 6-species system, ZOO3 and BIV4 are the principal phytoplankton-eating animals in the 19 species system.

We built for each solution of the optimisation problem and different goal function a dynamical system and estimate the stability of the fixed point. The maximum of the real parts of the eigenvalues of the Jacobians are reported in Table 4, similar to Table 3. All the flows correspond to an unstable fixed point showing that the constraints may need to be refined.

We also examined the ecosystems studied in [43]. For all the cases, the biomass fixed point was found to be stable. For many ecosystems, as for example the Crystal River Creek in [43], the detritus component has a large biomass. This induces stability, as was shown above.

Above methods may also be applied to human environmental networks, or in economics, for example to economic resource trade flow networks; see [20], [16], and the references therein.

To conclude, we introduced a methodology to study the possible flows of an ecosystem defined by observational biomass data and realistic biological constraints. We formalized the constraints and described precisely the polytope containing the solutions. We presented a convex optimization problem based

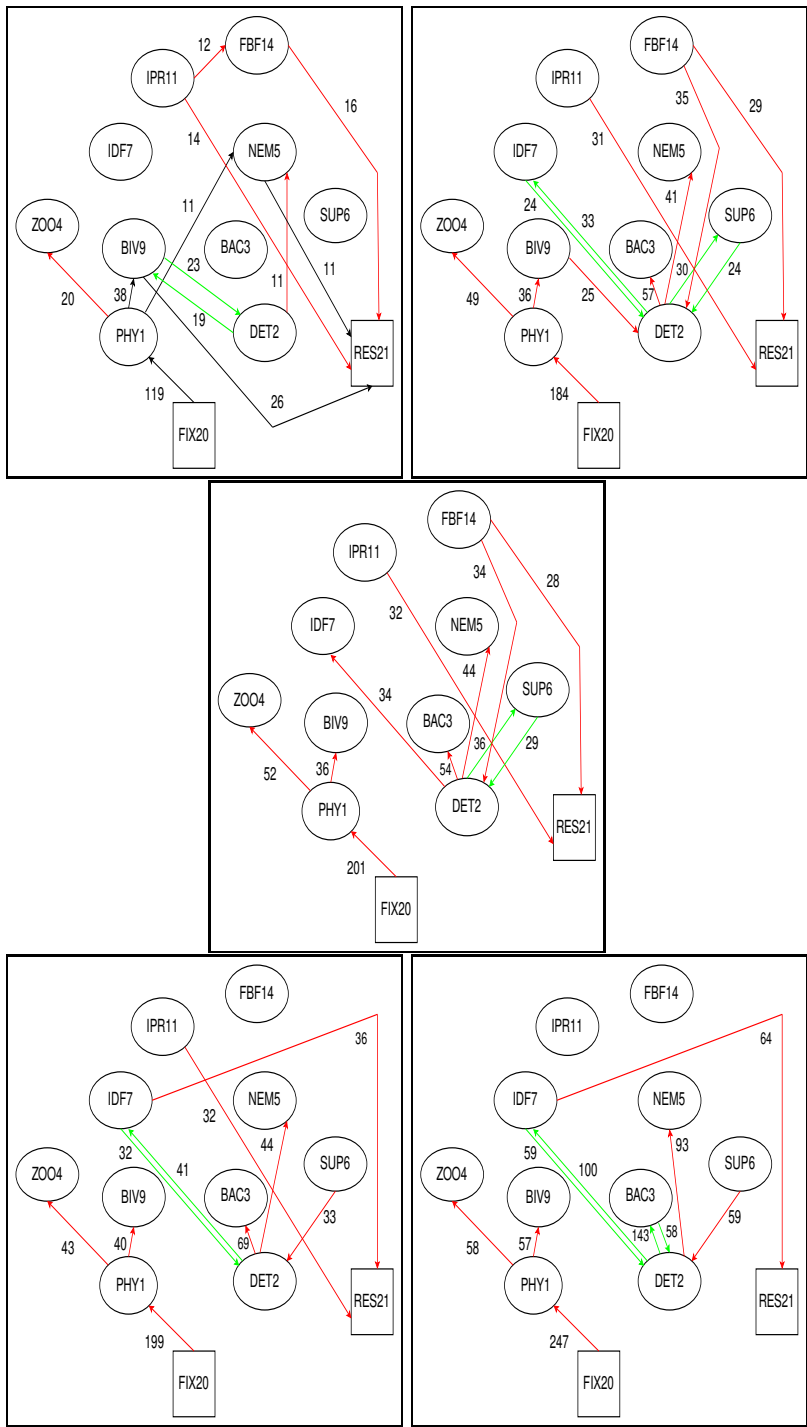


Figure 5: The largest flows for the goal functions: **top** F_1 (left) and F_2 (right), **middle** F_3 , **bottom** F_4 (left) and F_5 (right).

on ecological network indices used as goal functions. The method is fast, can be used for large systems and provides a solution within the polytope according to the indices.

The minimal flow for each goal function can be analyzed using two different complementary tools. First, the flow is decomposed into principal paths and circuits. These enable ecologists to discriminate between the different solutions. Second, the consistency of the flow is examined by introducing a dynamical system and studying the stability of the biomasses fixed point.

References

- [1] A. Belgrano, U.M. Scharler, J. Dunne, R.E. Ulanowicz, Aquatic food webs: an ecosystem approach Oxford Univ. Press. (2005).
- [2] P. T. Boggs, J. W. Tolle, Sequential Quadratic Programming, *Acta Numerica*, 4, 1-51 (1995)
- [3] T. Brey, Population dynamics in benthic invertebrates. A virtual handbook , Alfred Wegener Institute for Polar and Marine Research, Germany, (2001). <http://www.awi-bremerhaven.de/Benthic/Ecosystem/FoodWeb/Handbook/main.html>
- [4] X. Chen, Nonlinear constrained optimization in R and its application for sufficient dimension reduction and variable selection, dissertation Dr Philosophy, Athens, Georgia, USA (2016).
- [5] T. M. Cover and J. Thomas, *Elements of information theory*, 2nd edition, Wiley New York (2006).
- [6] V. Christensen, C.J. Walters, Ecopath with Ecosim: Methods, capabilities and limitations, *Ecol. Modell.* 172, 109–139 (2004).
- [7] I. Csiszar, I-divergence geometry of probability distributions and minimization problems *Annals Probab.* 3, 146-158, (1975).
- [8] J.-C. Dauvin and T. Ruellet, Macrozoobenthic biomass in the Bay of Seine (eastern English Channel) *Journal of Sea Research* 59, 320-326, (2008).
- [9] J.F. De Pierrepont, B. Dubois, S. Desormonts, M.B. Santos and J.P. Robin Stomach contents of English Channel cetaceans stranded on the coast of Normandy, *J. Mar. Biol. Ass. U.K.*, 85, 1539-1546 (2005).
- [10] C. Fontaine, P.R. Guimaraes, S. Kéfi, N. Loeuille, J. Memmott, W.H. van der Putten, F.J.F. van Veen, E. Thébault, The ecological and evolutionary implications of merging different types of networks , *Ecol. Lett.* 14, 1170–1181 (2011).
- [11] R. Froese and D. Pauly, FishBase, version 10/2004, Los Banos. (2004). <http://www.fishbase.org>

- [12] S. Frontier and D. Pichod-Viale, *Ecosystèmes-structures-fonctionnement-évolution*, Masson, Paris, Coll. d'écologie, 21, (1991).
- [13] G.T. Gilbert, Positive Definite Matrices and Sylvester's Criterion, *The American Mathematical Monthly*, 98, 44-46 (1991).
- [14] B. S. Goh, Global stability in many species systems, *The American Naturalist*, 111, 135-143, (1977).
- [15] H. Hirata and R. E. Ulanowicz, Large-scale systems perspective on ecological modelling and analysis , *Ecol. Modell.* 31, 79-104 (1986).
- [16] J. Huang¹, R. E. Ulanowicz^{2,3}, Ecological Network Analysis for Economic Systems: Growth and Development and Implications for Sustainable Development, *PLoS ONE* 9, e100923 (2014).
- [17] G. E. Hutchinson, *The kindly fruits of the earth: recollections of an embryocologist*. Yale University Press, New Haven (1979).
- [18] S. Johnson, V. Dominguez-Garcia, L. Donetti, M. A. Munoz, Trophic coherence determines food-web stability, *Proc Natl Acad Sci U S A.* 111, 17923-17928 (2014).
- [19] S.E. Jørgensen, B.D. Fath, *Fundamentals of ecological modelling: Applications in environmental management and research*, Elsevier Amsterdam (2011).
- [20] A. Kharrazi, E. Rovenskaya, B. D. Fath, M. Yarime, S. Kraines, Quantifying the sustainability of economic resource networks: An ecological information-based approach, *Ecological Economics* 90, 177–186 (2013).
- [21] J.K. Kones, K. Soetaert, D. van Oevelen, J.O. Owino, K. Mavuti, Gaining insight into food webs reconstructed by the inverse method , *J. Mar. Syst.* 60, 153–166 (2006).
- [22] J.K. Kones, K. Soetaert, D. van Oevelen, J.O. Owino, Are network indices robust indicators of food web functioning? A Monte Carlo approach , *Ecol. Modell.* 220, 370–382 (2009).
- [23] S. Kullback, R.A. Leibler On Information and Sufficiency, *Annals Math. Stat.* 22, 79–86 (1951).
- [24] D. Langlet, R. Rayfuse, *The Ecosystem Approach in Ocean Planning and Governance*, Brill Nijhoff, Leiden (2018).
- [25] L.G. Latham, Network flow analysis algorithms. *Ecol. Modell.* 192, 586–600 (2006).
- [26] R. L. Lindeman The Trophic-Dynamic Aspect of Ecology, *Ecology*, 23, 399-417, (1942).

- [27] D. Luenberger, Introduction to dynamic systems, J. Wiley, New York (1979).
- [28] R.H., MacArthur, Fluctuations of animal populations and a measure of community stability. *Ecology*, 36, 533-536 (1955).
- [29] J. D. Murray, *Mathematical Biology V2*, Springer Berlin (2003).
- [30] C. Napoléon, P. Claquin, Multi-Parametric Relationships between PAM Measurements and Carbon Incorporation, an In Situ Approach, *Plos One*, 7, e40284, (2012).
- [31] G. Nemhauser and L. Wolsey, *Integer and Combinatorial Optimization*, Wiley New York (1988).
- [32] N. Niquil, B. Saint-Béat, G.A. Johnsin, K. Soetaert, D. van Oevelen, C. Bacher, A.F. Vézina, Inverse Modeling, in *Modern Ecology and Application to Coastal Ecosystems*, Elsevier Amsterdam (2011).
- [33] Q. Noguès, A. Raoux, E. Araignous, T. Hattab, B. Leroy, F. Ben Rais Lasram, F. Le Loc'h, J. Dauvin, N. Niquil, Cumulative effects of marine renewable energy and climate change on ecosystem properties: Sensitivity of ecological network analysis, *Ecol. Indic.*, to appear (2020). <https://doi.org/10.1016/j.ecolind.2020.107128>.
- [34] E.P. Odum, *Fundamentals of ecology*, W.B. Saunders Company, Philadelphia (1953).
- [35] E.P. Odum, The Strategy of Ecosystem Development, *Science* 164, 262–270 (1969).
- [36] B.C. Patten, *Systems Analysis and Simulation in Ecology*. Academic Press, New York and London (1972).
- [37] H. Rybarczyk and B. Elkaim, An analysis of the trophic network of a macrotidal estuary: the Seine Estuary (Eastern Channel, Normandy, France) *Estuarine, Coastal and Shelf Science*, 58, 775-791, (2003).
- [38] B. Saint-Béat, A.F. Vézina, R. Asmus, H. Asmus, N. Niquil, The mean function provides robustness to linear inverse modelling flow estimation in food webs: A comparison of functions derived from statistics and ecological theories, *Ecol. Modell.* 258, 53–64 (2013).
- [39] A. C. Scott, *Nonlinear Science: Emergence and Dynamics of Coherent Structures*, Oxford Texts in Applied and Engineering Mathematics (1999).
- [40] A. G. Tansley, The Use and Abuse of Vegetational Concepts and Terms, *Ecology*, 16, 284-307, (1935).
- [41] R. E. Ulanowicz, *Growth and Development: Ecosystems Phenomenology*, Springer New York, (1986).

- [42] R. E. Ulanowicz, Ecology, the ascendent perspective, Columbia University Press (1997).
- [43] R. E. Ulanowicz, Biodiversity, functional redundancy and system stability: subtle connections, J. R. Soc. Interface, 15, 2018.0367 (2018).
- [44] K. Van den Meersche, K. Soetaert, D. Van Oevelen, xsample(): An R Function for Sampling Linear Inverse Problems, J. Stat. Softw. 30 (2009).
- [45] D. Van Oevelen, K. Van den Meersche, F. J. R. Meysman, K. Soetaert, J. J. Middelburg, A. F. Vézina, Quantifying Food Web Flows Using Linear Inverse Models, Ecosystems 13, 32-45 (2010).
- [46] A. Vézina, T. Platt, Food web dynamics in the ocean. I. Best-estimates of flow networks using inverse methods , Mar. Ecol. Prog. Ser. 42, 269–287 (1988).

8 Appendix

Appendix 1: SQL local algorithm of Section 4.2

The SQL local algorithm solves a nonlinear minimization problem under constraints, say:

$$\begin{aligned} \min_f \quad & F(f), \\ h_i(f) = 0, \quad & i = 1, \dots, m, \\ g_j(f) \leq 0, \quad & j = 1, \dots, n. \end{aligned}$$

Let $\mathcal{L}(f, \alpha, \beta) = F(f) - \alpha^T h(f) + \beta^T g(f)$ denote the Lagrangian function of this problem where α and β are Lagrange multipliers of dimensions m and n respectively. Let \mathcal{W} denote the Hessian matrix of \mathcal{L} , defined by

$$\mathcal{W}_k \equiv \mathcal{W}(f_k, \alpha_k, \beta_k) = \nabla_{ff}^2 \mathcal{L}(f_k, \alpha_k, \beta_k),$$

and $\mathcal{A}(f)$ the Jacobian matrix of the constraints,

$$\mathcal{A}(f)^T = [\nabla h_1(f), \dots, \nabla h_m(f), \nabla g_1(f), \dots, \nabla g_n(f)].$$

Since the cost function F is convex, \mathcal{W}_k is a positive definite matrix and $\mathcal{A}(f)$ is a full rank matrix. Then, at an iterate f_k , a basic sequential quadratic programming algorithm defines an appropriate search direction p_k as a solution to the quadratic programming subproblem

$$\begin{aligned} \min_p \quad & \frac{1}{2} p^T \mathcal{W}_k p + \nabla f_k^T p, \\ \nabla h_i(f_k)^T p + h_i(f_k) = 0, \quad & i = 1, \dots, m, \\ \nabla g_j(f_k)^T p + g_j(f_k) = 0, \quad & j = 1, \dots, n. \end{aligned}$$

This is solved by the following algorithm:

Goal function	Computing time	function evaluations
F_1	0.2s	127
F_2	0.3s	2002
F_3	0.4s	2118
F_4	0.3s	2901
F_5	0.2s	307
Goal function	Computing time	function evaluations
F_1	0.9s	583
F_2	7s	55684
F_3	12s	60905
F_4	9s	78447
F_5	1s	1742

Table 5: Computing times and function evaluations: **top** 6-species system; **bottom** 19-species system

1. Take the initial points (f_0, α_0, β_0) ;
2. **For** $k = 0, 1, 2, 3, \dots$
 - Evaluate $F_{f_k}, \nabla F_{f_k}, \mathcal{W}_k = \mathcal{W}(f_k, \alpha_k, \beta_k), h_k, g_k, \nabla h_k$ and ∇g_k ;
 - Solve the quadratic subproblem for obtaining p_k, α_k, β_k ;
 - $f_{k+1} \leftarrow f_k + p_k; \alpha_{k+1} \rightarrow u_k; \beta_{k+1} \rightarrow v_k$;
 - If** the condition of convergence is satisfied;
 - STOP** with the approximate solution;
3. **End(For)**.

The computing time on an Intel I7 processor and number of function calls are given in Table 5. The code will be made available on github.

Appendix 2: Convexity of goal functions

In this appendix, we show that all the goal functions considered in Section 4.1 are convex.

Both F_1 and F_5 are sums of squares so they are obviously convex. Further, if a function is twice continuously differentiable, then it is convex if and only if its Hessian is positive semidefinite. We therefore calculate the Hessians \mathcal{H}_i of F_i for $i=2, 3, 4$. First

$$\mathcal{H}_2 = \mathcal{H}_4 = \begin{bmatrix} \frac{1}{p^{i,j}} & 0 & \dots & 0 \\ 0 & \frac{1}{p^{k,l}} & \dots & 0 \\ \dots & \dots & \dots & \dots \\ 0 & 0 & \dots & \frac{1}{p^{r,s}} \end{bmatrix},$$

that is obviously positive definite. This shows that indeed the entropy F_2 and the Kullback Leibler divergence F_4 are convex.

Let us rewrite the redundancy F_3 as

$$F_3 = \sum_{(i,j) \in E} p_{i,j} \ln \left(\frac{p_{i,j}}{p_{i.}} \right) + \sum_{(i,j) \in E} p_{i,j} \ln \left(\frac{p_{i,j}}{p_{.j}} \right).$$

The goal is to show that each term $T_{ij}^1 \equiv p_{i,j} \ln \left(\frac{p_{i,j}}{p_{i.}} \right)$ is convex. The Hessian of T_{ij}^1 is

$$\mathcal{H}_{ij} = \begin{bmatrix} \frac{(p_{i.} - p_{i,j})^2}{p_{i,j} p_{i.}^2} & -\frac{p_{i.} - p_{i,j}}{p_{i.}^2} & \cdots & -\frac{p_{i.} - p_{i,j}}{p_{i.}^2} \\ -\frac{p_{i.} - p_{i,j}}{p_{i.}^2} & \frac{p_{i,j}}{p_{i.}^2} & \cdots & \frac{p_{i,j}}{p_{i.}^2} \\ \cdots & \cdots & \cdots & \cdots \\ -\frac{p_{i.} - p_{i,j}}{p_{i.}^2} & \frac{p_{i,j}}{p_{i.}^2} & \cdots & \frac{p_{i,j}}{p_{i.}^2} \end{bmatrix}$$

Let us use the Sylvester's criterion to show that T_{ij}^1 is convex; see [13]. This criterion says that a Hermitian matrix is positive semidefinite if and only if all of its leading principal minors are positive.

The Hessian \mathcal{H}_{ij} is a Hermitian matrix. Let M_{ij}^k denote the principal minors of this Hessian. We have :

$$M_{ij}^1 = \frac{(p_{i.} - p_{i,j})^2}{p_{i,j} p_{i.}^2} \geq 0 \quad \text{and} \quad M_{ij}^2 = \det \begin{bmatrix} \frac{(p_{i.} - p_{i,j})^2}{p_{i,j} p_{i.}^2} & -\frac{p_{i.} - p_{i,j}}{p_{i.}^2} \\ -\frac{p_{i.} - p_{i,j}}{p_{i.}^2} & \frac{p_{i,j}}{p_{i.}^2} \end{bmatrix} = 0.$$

Moreover, $M_{ij}^k = 0$ for all $k \geq 3$, because then M_{ij}^k has at least two equal lines (or columns). Therefore, the Sylvester's criterion is satisfied and each term T_{ij}^1 is convex.

Similarly, each term $T_{ij}^2 \equiv p_{i,j} \ln \left(\frac{p_{i,j}}{p_{.j}} \right)$ is also convex, and hence F_3 is convex as a sum of convex terms.

Let us now show, using a counter-example that the ascendancy, defined by [15] as

$$A(f) = \sum_{ij \in E} \frac{f_{i,j}}{f_{..}} \ln \left(\frac{f_{i,j} f_{..}}{f_{i.} f_{.j}} \right)$$

is not convex. In this aim, consider the graph with three flows f_{12} , f_{23} and f_{13} shown on Fig. 6.

We compute

$$A = f_{13} \ln \left(\frac{f_{13}}{(f_{13} + f_{12})(f_{23} + f_{13})} \right) - f_{23} \ln(f_{23} + f_{13}) - f_{12} \ln(f_{13} + f_{12}).$$

The gradient of A is given by

$$\begin{aligned} A_{f_{12}} &= -\ln(f_{13} + f_{12}) - 1, & A_{f_{23}} &= -\ln(f_{13} + f_{23}) - 1, \\ A_{f_{13}} &= \ln \left(\frac{f_{13}}{f_{13}^2 + (f_{23} + f_{12}) f_{13} + f_{12} f_{23}} \right) - 1. \end{aligned}$$

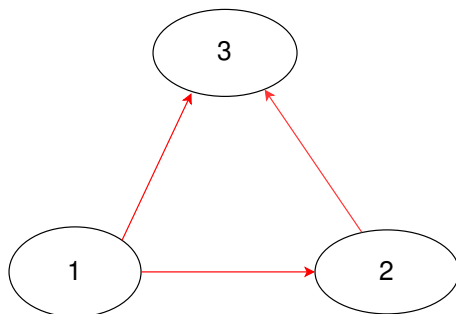


Figure 6: Example of 3-species model ecosystem

There is only one extremum, $f_{12} = f_{23} = 0$ and $f_{13} = e^{-1} \approx 0.3678$.

The Hessian of A is

$$\mathcal{H}_A = \begin{pmatrix} -\frac{1}{f_{13}+f_{12}} & 0 & -\frac{1}{f_{13}+f_{12}} \\ 0 & -\frac{1}{f_{13}+f_{23}} & -\frac{1}{f_{13}+f_{12}} \\ -\frac{1}{f_{13}+f_{12}} & -\frac{1}{f_{13}+f_{23}} & -\frac{f_{13}^2 - f_{12} f_{23}}{f_{13}^3 + (f_{23} + f_{12}) f_{13}^2 + f_{12} f_{23} f_{13}} \end{pmatrix}.$$

For $f_{12} = 1, f_{23} = 1, f_{13} = 0.4$, we get

$$H = \begin{pmatrix} -0.714 & 0 & -0.714 \\ 0 & -0.714 & -0.714 \\ -0.714 & -0.714 & 1.0714 \end{pmatrix},$$

which is clearly not positive semidefinite.

Appendix 3: Lemma 8.1

A classical result is that the eigenvalues of a skew-symmetric real matrix are pure imaginary or zero. Indeed, let A be a skew-symmetric matrix and $B = iA$, then $B^* = -iA^T = iA = B$ and therefore B is Hermitian. Since B has all real eigenvalues $\lambda_1, \dots, \lambda_n$, all the eigenvalues of A are of the form $-i\lambda_1, \dots, -i\lambda_n$ and thus all pure imaginary.

The following modified version deserves to be proven.

Lemma 8.1 *Let J^0 be a matrix such that $J^0 = DA$, where D is diagonal with non zero elements and A is skew-symmetric. Then the eigenvalues of J^0 are either imaginary numbers or zero.*

proof

Let λ be an eigenvalue of J^0 . Let v be an associated eigenvector, such that

$DAv = \lambda v$. Since D is invertible, we have

$$Av = \lambda D^{-1}v. \quad (42)$$

First, the product of both sides of (42) with \bar{v}^T gives

$$\bar{v}^T Av = \lambda \bar{v}^T D^{-1}v. \quad (43)$$

Since $\lambda \bar{v}^T D^{-1}v$ is a scalar, taking transpose of both sides of (43) yields $(Av)^T \bar{v} = -v^T A\bar{v}$, and hence

$$\lambda \bar{v}^T D^{-1}v = (Av)^T \bar{v} = -v^T A\bar{v}. \quad (44)$$

Second, the complex conjugate of (42) is $A\bar{v} = \bar{\lambda} D^{-1}\bar{v}$. The product of both sides with v gives

$$v^T A\bar{v} = \bar{\lambda} v^T D^{-1}\bar{v}. \quad (45)$$

Finally, since $v^T D^{-1}\bar{v} = (D^{-1}\bar{v}, v) = (D^{-1}v, v) > 0$, identifying the two expressions of $v^T A\bar{v}$ in (44) and (45) yields $\lambda = -\bar{\lambda}$, so that λ is a pure imaginary number or zero, and the lemma is proven.